The impact of deniers on epidemics: A temporal network model

The impact of deniers on epidemics: A temporal network model

Lorenzo Zino, *Member, IEEE*, Alessandro Rizzo, *Senior Member, IEEE*, and Maurizio Porfiri, *Fellow, IEEE*

***Abstract*— We propose a novel network epidemic model to elucidate the impact of deniers on the spread of epidemic diseases. Specifically, we study the spread of a recurrent epidemic disease, whose progression is captured by a susceptible–infected–susceptible model, in a population partitioned into two groups: cautious and deniers. Cautious individuals may adopt self-protective behaviors, possibly incentivized by information campaigns implemented by public authorities; on the contrary, deniers reject their adoption. Through a mean-field approach, we analytically derive the epidemic threshold for large-scale homogeneous networks, shedding light onto the role of deniers in shaping the course of an epidemic outbreak. Specifically, our analytical insight suggests that even a small minority of deniers may jeopardize the effort of public health authorities when the population is highly polarized. Numerical results extend our analytical findings to heterogeneous networks.**

***Index Terms*— Network analysis and control; Control of networks**

I. Introduction

MATHEMATICAL models of epidemic spreading on networks have gained increasing popularity in the last decade. They have emerged as powerful tools to predict the course of epidemic outbreaks [1]–[6] and, ultimately, to design and assess intervention policies [2], [5], [7]. In the last few years, the COVID-19 global health crisis has provided further motivation to pursue these studies. Within this collective effort, the systems and control community has worked toward developing new models to capture specific features of COVID-19 [8]. Through the lens of network theory, effective tools to predict the spread of the disease and assess the effectiveness of different intervention policies were developed [9]–[11].

However, there are still significant gaps in the application of network theory to study epidemics, particularly in the context of modeling human behavior. Human behavior plays a crucial role in shaping the course of an epidemic outbreak, as the individuals' response to the epidemic spreading may be quite diverse across a population [12]. In fact, while the majority of the individuals were concerned by the COVID-19 pandemics and were keen to adopt self-protective measures to avoid the contagion, a nonnegligible minority of individuals kept denying the severity of the pandemic, or even its existence [13]. They refused to take any action against the contagion, even to comply with compulsory measures enforced by public authorities, such as social distancing or the use of face masks [14]. The behavioral response to a pandemic is indeed a divisive topic [15], which may lead to the emergence or the increase of polarization in the pattern of social interactions, since people might prefer to interact with like-minded individuals [16]. The extent to which the presence of deniers and the emergence of polarization impact the pandemic spreading and the effectiveness of information campaigns is still unclear, despite its paramount importance.

In this letter, we investigate these questions by proposing a novel model for the spread of recurrent diseases, accounting for the presence of deniers. Specifically, we design a temporal network model in which the population is partitioned into two groups: cautious individuals and deniers. While cautious individuals may decide to adopt self-protective behaviors to prevent contagion, possibly encouraged by information campaigns, deniers always refuse to adopt these behaviors. Interactions between and within these groups are regulated by a parameter, termed homophily, which captures the tendency of individuals to interact with like-minded people.

Formally, we develop our model within the continuous-time activity-driven network (ADN) paradigm [17], and we expand such a framework to account for the population structure. The use of ADNs allows us to formalize a model that is analytically tractable and amenable to fast numerical simulations [18], [19]. We model the epidemic spreading using two distinct compartmental models. For deniers, we adopt the well-known susceptible–infected–susceptible (SIS) model; whereas, for cautious individuals, we employ a susceptible–alert–infected–susceptible (SAIS) model. The latter extends the SIS model by including an additional state to keep track of individuals who adopt self-protective behaviors to avoid contagion [19]–[21]. We assume that self-protective behaviors are always successful in preventing contagion, but they come with a nonnegligible cost that may drive people to abandon them. Hence, the adoption and rejection of self-protective behavior are regulated by two contrasting mechanisms that account for information campaigns implemented by public health authorities and the social economic costs associated with their use.

We expand on the mean-field approach proposed in [22] to study the epidemic model, accounting for heterogeneity in

L. Zino and A. Rizzo are with the Department of Electronics and Telecommunications, Politecnico di Torino, Torino, Italy ({lorenzo.zino,alessandro.rizzo}@polito.it). L. Zino was with the Engineering and Technology Institute Groningen, University of Groningen, Groningen, The Netherlands. A. Rizzo is also with the Institute for Invention, Innovation, and Entrepreneurship, New York University Tandon School of Engineering, Brooklyn NY, USA. M. Porfiri is with the Center for Urban Science and Progress, the Department of Mechanical and Aerospace Engineering, and the Department of Biomedical Engineering, New York University Tandon School of Engineering, Brooklyn NY 11201, USA (mporfiri@nyu.edu). This work was partially supported by National Science Foundation (CMMI-2027990).

the population. For large-scale networks, we study the local exponential stability of the disease-free equilibrium (DFE), which determines when self-protective behaviors are successful in preventing global outbreaks. For homogeneous ADNs, in which all the individuals have the same level of social activity, we analytically establish a closed-form expression for the epidemic threshold, shedding light onto the impact of deniers on the success on eradicating a local epidemic outbreak. Predictably, the presence of deniers favors the spread of epidemic diseases. Moreover, our analytical insight exposes the detrimental role played by polarization: in highly polarized networks, even small minorities of deniers can jeopardize the efforts of public health authorities in promoting self-protective behaviors. For heterogeneous ADNs, we derive a closed-form expression for the linearization of the system about the DFE, which allows for the fast numerical evaluation of the epidemic threshold. Our numerical findings suggest that heterogeneity may further favor the spread of epidemic diseases.

We gather here the notation used in the letter. We denote by $\mathbb{R}$, $\mathbb{R}_{\geq 0}$, $\mathbb{R}_{>0}$, and $\mathbb{Z}_{>0}$ the set of real, real nonnegative, strictly positive real, and strictly positive integer numbers, respectively. Given a continuous-time function $x(t)$, we define $x(t^-) := \lim_{s \nearrow t} x(s)$ and $x(t^+) := \lim_{s \searrow t} x(s)$. A Poisson clock with rate $\rho \in \mathbb{R}_{>0}$ is a continuous-time stochastic process that clicks once between time t and $t + \Delta t$ with probability $\rho \Delta t + o(\Delta t)$, independent of the past, where the Landau notation $o(\Delta t)$ is associated with the limit $\Delta t \searrow 0$.

II. Model

A. Population model

We consider a population of $n \in \mathbb{Z}_{>0}$ individuals, $\mathcal{V} = \{1, \dots, n\}$, partitioned in two sub-populations: the *deniers* and the *cautious* individuals. Deniers are not concerned about the disease spreading and refuse to adopt any self-protective measures, even if enforced by public authorities [14]. On the contrary, cautious individuals are worried about the epidemic disease, and they may decide to adopt self-protective behaviors. Without any loss in generality, we assume that $\mathcal{V}_d := \{1, \dots, n_d\}$ is the set of deniers, and $\mathcal{V}_c := \{n_d + 1, \dots, n\}$ contains the cautious individuals. The fraction of deniers is quantified by the parameter $\eta := n_d/n \in [0, 1]$.

Each individual $v \in \mathcal{V}$ is associated with a state $x_v(t)$ that evolves in continuous time ($t \in \mathbb{R}_{\geq 0}$) and characterizes the individual's health state and behavior. Specifically, all individuals can be either *susceptible* to the disease ($x_v(t) = \mathrm{S}$) or *infected* with the disease ($x_v(t) = \mathrm{I}$). Furthermore, cautious individuals may be associated with a third state, which accounts for the adoption of *self-protective* behaviors ($x_v(t) = \mathrm{P}$). Here, we assume that self-protective behaviors are ideal, so that their adoption is 100% effective in preventing contagion. However, their adoption is associated with social and economic costs that may push people to drop them.

B. Time-varying interaction network

Each individual is identified by a node in an undirected temporal network $(\mathcal{V}, \mathcal{E}(t))$, where the link set $\mathcal{E}(t)$ captures the evolving pattern of human-to-human interactions: $\{v, w\} \in \mathcal{E}(t)$ means that individuals v and w interact at time t. The temporal network is generated according to a stochastic mechanism, inspired by continuous-time ADNs [17], which we extend to account for the population structure. Specifically, each individual $v \in \mathcal{V}$ is characterized by a constant parameter $a_v \in \mathbb{R}_{>0}$, termed *activity*, which captures the individual's propensity to initiate interactions with others. We further introduce a parameter $\theta \in [0, 1]$, which captures the individuals' preference to interact with people sharing similar beliefs, termed *homophily* [16]: the larger θ, the more individuals tend to interact within their sub-population.

The network temporal is generated according to the following steps: i) at time $t = 0$, the link set is initialized as $\mathcal{E}(t) = \emptyset$. Each node $v \in \mathcal{V}$ is associated with a Poisson clock with rate equal to a_v, each one independent of the others; ii) time progresses until any of the n Poisson clocks involved in the process clicks; iii) if the clock associated with node $v \in \mathcal{V}$ clicks at time t, individual v is *activated* and selects a fellow individual w to interact with. The individual w is selected according to a probabilistic rule: with probability θ, w is selected uniformly at random among the individuals with the same belief of v (that is, among $\mathcal{V}_d$ if $v \in \mathcal{V}_d$, or among $\mathcal{V}_c$ if $v \in \mathcal{V}_c$); otherwise, w is selected uniformly at random in the entire population $\mathcal{V}$; iv) the undirected link $\{v, w\}$ is added to $\mathcal{E}(t)$; and v) the link is immediately removed from the set, the Poisson process associated with node v is reinitialized, and the process is resumed from item ii).

C. Epidemic model

The state of each individual $v \in \mathcal{V}$, $x_v(t)$, evolves according to two different epidemic progressions for deniers and cautious individuals. Deniers revise their state according to a standard SIS model [5], while cautious individuals follow an SAIS model [20], [21], implemented as in [19]. Both models involve *contagion* and *recovery*, while SAIS has two additional mechanisms: *awareness* and *unprotecting*, described in the following.

Contagion. If a susceptible individual v ($x_v(t^-) = \mathrm{S}$) contacts an infected one at time t ($(v, w) \in \mathcal{E}(t)$ with $x_w(t) = \mathrm{I}$), then v becomes infected ($x_v(t^+) = \mathrm{I}$) with probability $\lambda \in [0, 1]$, independent of the others.

Recovery. An infected individual ($x_v(t^-) = \mathrm{I}$) spontaneously recovers and becomes susceptible according to a Poisson clock with rate $\mu \in \mathbb{R}_{>0}$, independent of the others. If $v \in \mathcal{V}_c$ is cautious, then v adopts self-protective behaviors after recovery ($x_v(t^+) = \mathrm{P}$); whereas, if $v \in \mathcal{V}_d$ is a denier, v becomes susceptible again to the disease ($x_v(t^+) = \mathrm{S}$).

Awareness. We introduce a parameter $\gamma \in \mathbb{R}_{\geq 0}$ to quantify the effort exerted by public heath administrations in information campaigns (a control input). A cautious susceptible individual ($x_v(t^-) = \mathrm{S}$, $v \in \mathcal{V}_c$) starts adopting self-protective behaviors ($x_v(t^+) = \mathrm{P}$) according to a Poisson clock with rate γ, independent of the others.

Unprotecting. A cautious individual who is adopting self-protective behaviors ($x_v(t^-) = \mathrm{P}$) spontaneously abandons them due to the social and economic costs associated with them ($x_v(t^+) = \mathrm{S}$) according to a Poisson clock with rate $\nu \in \mathbb{R}_{>0}$, independent of the others. The rate ν captures the costs associated with the adoption of self protections.

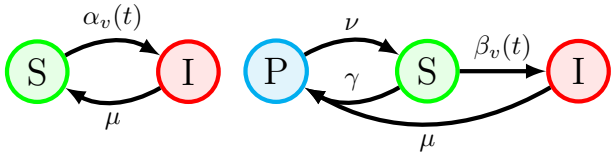

(a) $v \in \mathcal{V}_d$ (b) $v \in \mathcal{V}_c$

Fig. 1: Schematic of the state transitions of the model.

III. Dynamics

A. Markov process

The formation process of the temporal network and the four mechanisms described in Section II are all governed by Poisson processes, each one independent of the others. Hence, they induce an n-dimensional continuous-time Markov process $\mathbf{x}(t) = [x_1(t) \dots x_n(t)]$ over the state space $\{\mathrm{S}, \mathrm{I}\}^{n_d} \times \{\mathrm{S}, \mathrm{P}, \mathrm{I}\}^{n_c}$ [23]. Depending on the sub-population they belong to, individuals may undergo up to four distinct state transitions, illustrated in Fig. 1, which are triggered by the processes described in Section II. The three transitions triggered by recovery (from I to S or P), awareness (from S to P) and unprotecting (from P to S) involve only spontaneous mechanisms. Hence, the corresponding transition rates of the Markov process are given by the rates of the underlying Poisson process (μ, γ, and ν, respectively). Contagion, instead, involves an interaction between two individuals and is dependent on their health state. In the following, we explicitly compute the corresponding transition rate.

Proposition 1: Let us define the indicator function

$$I_v(t) := \begin{cases} 1 & \text{if } x_v(t) = \mathrm{I}, \\ 0 & \text{otherwise.} \end{cases} \tag{1}$$

A susceptible denier ($x_v(t^-) = \mathrm{S}$, $v \in \mathcal{V}_d$) becomes infected ($x_v(t^+) = \mathrm{I}$) according to a Poisson clock with rate

$$\alpha_v(\mathbf{x}(t)) := \lambda a_v \Big[\frac{\theta}{\eta n} \sum_{w \in \mathcal{V}_d} I_w(t) + \frac{1-\theta}{n} \sum_{w \in \mathcal{V}} I_w(t)\Big] + \lambda \Big[\frac{\theta}{\eta n} \sum_{w \in \mathcal{V}_d} a_w I_w(t) + \frac{1-\theta}{n} \sum_{w \in \mathcal{V}} a_w I_w(t)\Big], \tag{2a}$$

while, for a cautious individual, $v \in \mathcal{V}_c$, the rate is equal to

$$\beta_v(\mathbf{x}(t)) := \lambda a_v \Big[\frac{\theta}{(1-\eta)n} \sum_{w \in \mathcal{V}_c} I_w(t) + \frac{1-\theta}{n} \sum_{w \in \mathcal{V}} I_w(t)\Big] + \lambda \Big[\frac{\theta}{(1-\eta)n} \sum_{w \in \mathcal{V}_c} a_w I_w(t) + \frac{1-\theta}{n} \sum_{w \in \mathcal{V}} a_w I_w(t)\Big]. \tag{2b}$$

Proof: A susceptible denier v becomes infected if any of the following four chains of events occur: i) v activates, decides to restrain the interactions within the denier community (which occurs with probability θ), contacts an infected individual (which occurs with robability equal to the fraction of infected individuals in the community), and becomes infected (with probability λ); ii) v activates, decides not to restrain the interactions within its community, has a contact with an infected individual (which occurs with probability equal to the fraction of infected individuals in the entire population), and becomes infected; iii) any of the infected denier individuals activates, decides to interact within the denier community, has a contact with v, and infects them; or iv) any of the infected individuals in the network activates, decides to interact within the whole network, has a contact with v, and infects them.

Since all the events in each chain are independent, the rate corresponding to each chain of events is computed by multiplying the activity rate of the individual who activates by the probability of each event in the chain [24]. For instance, for chain i), we obtain the product $a_v \theta \frac{1}{\eta n} \sum_{w \in \mathcal{V}_d} I_w(t) \lambda$, which yields the first term in (2a). We recall that the transition occurs as soon as the fastest of the four chains of events occurs, and the events in the chains are disjoint. Hence, the transition is triggered by a Poisson clock with rate equal to the sum of the rates of the four chains [24]. After algebraic simplifications, we obtain (2a). A similar argument yields (2b). ∎

We can summarize the transition rates of the Markov process $\mathbf{x}(t)$ using the transition rate matrices

$$Q_v^d = \begin{bmatrix} \cdot & \alpha_v(\mathbf{x}(t)) \\ \mu & \cdot \end{bmatrix}, \quad Q_v^c = \begin{bmatrix} \cdot & \gamma & \beta_v(\mathbf{x}(t)) \\ \nu & \cdot & 0 \\ 0 & \mu & \cdot \end{bmatrix}, \tag{3}$$

that is, the probability that $v \in \mathcal{V}_s$ with $s \in \{d, c\}$ changes state from $h \in \{\mathrm{S}, \mathrm{P}, \mathrm{I}\}$ to $k \in \{\mathrm{S}, \mathrm{P}, \mathrm{I}\}$ is equal to $\mathbb{P}[x_v(t + \Delta t) = k \,|\, x_v(t) = h] = (Q_v^s)_{hk} \Delta t + o(\Delta t)$, for any $h \neq k$, with the understanding that P can only be reached if $v \in \mathcal{V}_c$.

B. Mean-field dynamics

Following [22], we consider a continuous-state deterministic mean-field relaxation of the dynamics in which, instead of the evolution of the individuals' state, we study its mean dynamics, in terms of the probability for each individual to be in each state. That is, for all $v \in \mathcal{V}$, we define

$$s_v(t) := \mathbb{P}[x_v(t) = \mathrm{S}], \quad i_v(t) := \mathbb{P}[x_v(t) = \mathrm{I}], \tag{4a}$$

while, for $v \in \mathcal{V}_c$, we further define

$$p_v(t) := \mathbb{P}[x_v(t) = \mathrm{P}]. \tag{4b}$$

Briefly, in the mean-field approach [22], the system dynamics is obtained by approximating the expected value of the transition rate matrices in (3) with the transition rate matrices for the expected state of the system ($\mathbb{E}[Q_v^d(\mathbf{x}(t))] \approx Q_v^d[\mathbb{E}[\mathbf{x}(t)]]$). Using this approach, the temporal evolution of the probabilities in (4) is approximated by a system of $2n + n_c$ ordinary differential equations (ODEs), obtained as $[\dot{s}_v\, \dot{i}_v] = [s_v\, i_v] Q_v^d[\mathbb{E}[\mathbf{x}(t)]]$, $\forall\, v \in \mathcal{V}_d$ and $[\dot{s}_v\, \dot{p}_v\, \dot{i}_v] = [s_v\, p_v\, i_v] Q_v^c[\mathbb{E}[\mathbf{x}(t)]]$, $\forall\, v \in \mathcal{V}_p$, recalling that $\mathbb{E}[I_w(t)] = i_w(t)$. For $v \in \mathcal{V}_d$, we obtain

$$\dot{s}_v = \mu i_v - s_v \bar{\alpha}_v, \tag{5a}$$

$$\dot{i}_v = -\mu i_v + s_v \bar{\alpha}_v, \tag{5b}$$

with

$$\bar{\alpha}_v := \lambda a_v \left[\frac{\theta}{\eta n} \sum_{w \in \mathcal{V}_d} i_w + \frac{1-\theta}{n} \sum_{w \in \mathcal{V}} i_w\right] + \lambda \left[\frac{\theta}{\eta n} \sum_{w \in \mathcal{V}_d} a_w i_w + \frac{1-\theta}{n} \sum_{w \in \mathcal{V}} a_w i_w\right], \tag{6}$$

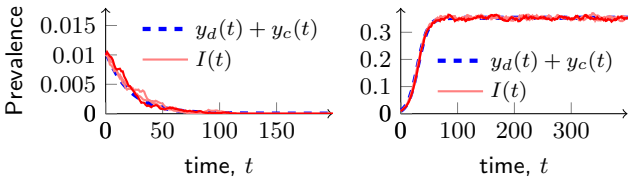

(a) $\gamma = 0.5$ (b) $\gamma = 0.2$

Fig. 2: Comparison between the Markov process and its deterministic approximation. Blue dashed curves are the epidemic prevalence computed integrating numerically (5) and (7); red solid curves are the epidemic prevalence in three runs of the Markov process. Common parameters: $n = 20,000$, $\eta = 0.1$, $\lambda = 0.06$, $\mu = 1/7$, $\nu = 0.5$, $\theta = 0.2$, and $a_v = 1$, $\forall\, v \in \mathcal{V}$.

and, for $v \in \mathcal{V}_c$, we obtain

$$\dot{s}_v = -\gamma s_v + \nu p_v - \bar{\beta}_v, \tag{7a}$$
$$\dot{p}_v = \gamma s_v - \nu p_v + \mu i_v, \tag{7b}$$
$$\dot{i}_v = -\mu i_v + s_v \bar{\beta}_v, \tag{7c}$$

with

$$\begin{aligned}\bar{\beta}_v := \lambda a_v \Big[\tfrac{\theta}{(1-\eta)n} \textstyle\sum_{w\in\mathcal{V}_c} i_w + \tfrac{1-\theta}{n} \sum_{w\in\mathcal{V}} i_w\Big] \\ +\lambda \Big[\tfrac{\theta}{(1-\eta)n} \textstyle\sum_{w\in\mathcal{V}_c} a_w i_w + \tfrac{1-\theta}{n} \sum_{w\in\mathcal{V}} a_w i_w\Big].\end{aligned} \tag{8}$$

The following result proves that (5) and (7) are well defined.

Lemma 1: The domain $\mathcal{S} := \{(s_v, i_v) : s_v, i_v \geq 0, s_v + i_v = 1\}^{n_d} \times \{(s_v, i_v) : s_v, p_v, i_v \geq 0, s_v + p_v + i_v = 1\}^{n_c}$ is positive invariant under (5) and (7).

Proof: We immediately verify that, if one of the variables is equal to 0, then its derivative is always nonnegative. Hence, the nonnegative orthant is a positive invariant set. We further observe that, under (5), $\dot{s}_v + \dot{i}_v = 0$, while under (7), $\dot{s}_v + \dot{p}_v + \dot{i}_v = 0$, preserving the sum of the variables for each node v, which proves our claim. ∎

Remark 1: As a consequence of Lemma 1, only $n + n_c$ of the ODEs from (5) and (7) are linearly independent.

From the set of $n + n_c$ independent ODEs that govern the mean-field evolution of the process, it is straightforward to conclude that the system has a unique DFE, that is, an equilibrium of (5) and (7) with $i_v = 0$ for all $v \in \mathcal{V}$. The DFE is characterized in the following lemma, proved by checking the equilibrium conditions for (5).

Lemma 2: The unique DFE of the system has $i_v = 0$ for all $v \in \mathcal{V}$ and $p_v = \frac{\gamma}{\gamma+\nu}$, for all $v \in \mathcal{V}_c$.

Before our main results, we introduce some more notation. Specifically, we define three macroscopic variables:

$$y_d := \frac{1}{n}\sum_{v\in\mathcal{V}_d} i_v,\ y_c := \frac{1}{n}\sum_{v\in\mathcal{V}_c} i_v,\ y_p := \frac{1}{n}\sum_{v\in\mathcal{V}_c} p_v, \tag{9}$$

that is, the average probability for a randomly selected node to be an infected denier, an infected cautious individual, and to adopt self-protective behaviors, respectively.

In the thermodynamic limit, $n \to \infty$, the temporal evolution of the stochastic process at the population level can be approximated by the macroscopic variables in (9) over any finite time-horizon with arbitrary accuracy [22], [25]. In particular, we can approximate the epidemic prevalence $I(t) := \frac{1}{n}|\{j \in \mathcal{V} : x_j(t) = \mathrm{I}\}| \approx y_d(t) + y_c(t)$, as illustrated in Fig. 2, which shows the high quality of the approximation even for medium-size networks.

IV. Results

A. Analytical results for the homogeneous ADNs

In general, it is not possible to derive closed-form expressions for the three ODEs that govern the macroscopic variables in (9). In fact, the temporal evolution of the average probabilities in (9) depends recursively on higher-order moments. However, closed-form expressions can be derived for specific, yet interesting cases. In the following, we make the assumption of homogeneous ADNs, in which all the individuals have the same activity.

Proposition 2: In the thermodynamic limit, $n \to \infty$, and if $a_v = a$, for all $v \in \mathcal{V}$, the mean-field evolution of the system of macroscopic equations in (9) is governed by

$$\begin{aligned}\dot{y}_d =& -\mu y_d + 2\lambda a(\eta - y_d)\cdot \\ &\cdot \Big[\big(1 + \theta\tfrac{1-\eta}{\eta}\big)y_d + (1-\theta)y_c\Big],\end{aligned} \tag{10a}$$
$$\begin{aligned}\dot{y}_c =& -\mu y_c + 2\lambda a(1 - \eta - y_c - y_p)\cdot \\ &\cdot \Big[\big(1 + \theta\tfrac{\eta}{1-\eta}\big)y_c + (1-\theta)y_d\Big],\end{aligned} \tag{10b}$$
$$\dot{y}_p = \gamma(1 - \eta - y_c - y_p) - \nu y_p + \mu y_c. \tag{10c}$$

Proof: First, we compute the derivative of (9) and we substitute (5b), obtaining

$$\dot{y}_d = \tfrac{1}{n}\sum_{v\in\mathcal{V}_d} \dot{i}_v = -\mu y_d + \tfrac{1}{n}\sum_{v\in\mathcal{V}_d}(1 - i_v)\bar{\alpha}_v. \tag{11}$$

Then, (10a) is obtained by observing that, if $a_v = a$, for all $v \in \mathcal{V}$, (6) reduces to $\bar{\alpha}_v = 2\lambda a[(1 + \theta\frac{1-\eta}{\eta})y_d + (1-\theta)y_c]$, which can be substituted into (11), leading to (10a). The other two equations come from similar arguments. ∎

Proposition 2 establishes that, for homogeneous ADNs, the epidemic spreading process can be studied with a three-dimensional nonlinear system of ODEs in (10), instead of the higher dimensional system in (5) and (7). The analysis of such a system allows us to compute the epidemic threshold, that is, to determine whether a local outbreak is eradicated, or if it becomes endemic. Formally, the epidemic threshold determines the region of the parameter space in which the DFE is (locally) exponentially stable.

Theorem 1: The system in Proposition 2 admits a locally exponentially stable DFE if and only if (iff)

$$\begin{aligned}\frac{\lambda}{\mu} < \sigma := \frac{1}{a}\Big[\eta(1-\theta) + \theta + \tfrac{\nu(1-\eta(1-\theta))}{\gamma+\nu} + \\ + \sqrt{\big(\eta(1-\theta) + \theta + \tfrac{\nu(1-\eta(1-\theta))}{\gamma+\nu}\big)^2 - 4\tfrac{\nu}{\gamma+\nu}\theta}\Big]^{-1}.\end{aligned} \tag{12}$$

Proof: First, we perform the change of variable $z = y_p - \frac{(1-\eta)\gamma}{\gamma+\nu}$, and we observe that the DFE of (9) coincides with the origin of the new system made by variables y_d, y_c, and z. We linearize this system about the origin, obtaining:

$$\dot{y}_d = -\mu y_d + 2\lambda a\eta\big[(1 + \theta\tfrac{1-\eta}{\eta})y_d + (1-\theta)y_c\big], \tag{13a}$$
$$\dot{y}_c = -\mu y_c + 2\lambda a\tfrac{\nu(1-\eta)}{\gamma+\nu}\big[(1 + \tfrac{\eta\theta}{1-\eta})y_c + (1-\theta)y_d\big], \tag{13b}$$
$$\dot{z} = \gamma(1 - \eta - y_c - z - \tfrac{(1-\eta)\gamma}{\gamma+\nu}) - \nu(z + \tfrac{(1-\eta)\gamma}{\gamma+\nu}) + \mu y_c. \tag{13c}$$

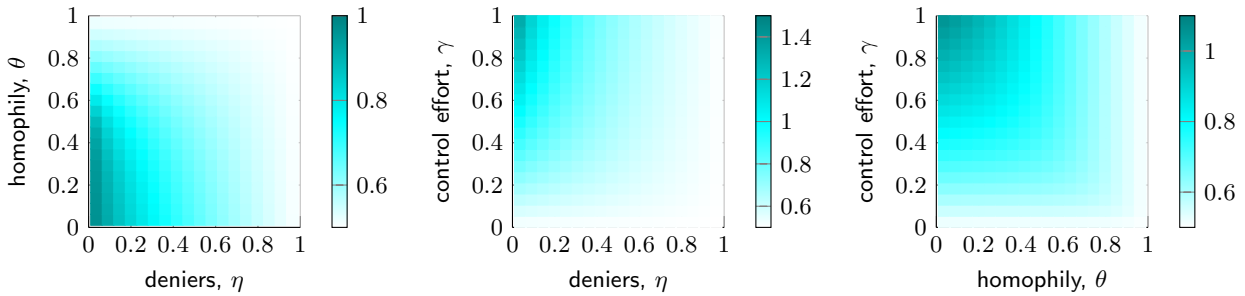

(a) $\gamma = 0.5$ (b) $\theta = 0.2$ (c) $\eta = 0.2$

Fig. 3: Threshold σ computed via (12) for different values of homophily, θ, fraction of deniers, η, and effort placed by public heath authorities in information campaigns, γ. Common parameters are $\nu = 0.5$ and $a_v = 1$, for all $v \in \mathcal{V}$.

The Jacobian matrix of (13) has a block-diagonal structure, which allows us to compute its three eigenvalues $\Lambda_{1,2,3}$. From the block associated with the third row of (13), we obtain the $\Lambda_1 = -\gamma - \nu < 0$. The other two eigenvalues are equal to $\Lambda_{2,3} = -\mu + \lambda a[\eta(1-\theta) + \theta + \frac{\nu(1-\eta(1-\theta))}{\gamma+\nu} \pm \sqrt{(\eta(1-\theta) + \theta + \frac{\nu(1-\eta(1-\theta))}{\gamma+\nu})^2 - 4\frac{\nu}{\gamma+\nu}\theta}]$ and are always real, since the square root can be cast as the sum of two non-negative quantities. Hence, the DFE is locally exponentially stable if all the eigenvalues of the Jacobian matrix of (13) evaluated in the origin are negative [26], which occurs iff (12) holds true, which concludes the proof. ∎

Remark 2: For $\theta = 0$, (12) reduces to $\lambda/\mu < [2a(\eta + \frac{\nu(1-\eta)}{\nu+\gamma})]^{-1}$. In the absence of deniers, $\eta = 0$, it further reduces to the threshold for a SAIS on a homogeneous ADN [19].

Our theoretical result in Theorem 1 allows us to shed light on the impact of deniers on the spread of epidemics. In Fig. 3, we report a parametric study for the epidemic threshold computed analytically using (12). Figure 3a shows that, while increasing the fraction of deniers predictably favors the epidemic spreading, also homophily has a strong impact: as θ increases, the threshold quickly decreases. This suggests that even a small minority of deniers could hinder the eradication of a disease in highly polarized scenarios. Figures 3b and 3c investigate the effectiveness of information campaigns in increasing the epidemic threshold, confirming that a small minority of deniers is able to jeopardize even large control efforts. For instance, in Fig. 3c, we observe that with only 20% of deniers, increasing the control effort has a marginal effect if the homophily is higher than $\theta = 0.5$.

B. Numerical results for heterogeneous ADNs

Despite the impossibility to derive closed-form expressions for heterogeneous ADNs, we can follow [17], [19] to establish a closed-form expression for the linearization of the system about the DFE, through some ancillary variables.

Proposition 3: Let us define

$$z_d := \frac{1}{n}\sum\nolimits_{v\in\mathcal{V}_d} i_v a_v, \quad z_c := \frac{1}{n}\sum\nolimits_{v\in\mathcal{V}_c} i_v a_v. \tag{14}$$

In the thermodynamic limit, $n \to \infty$, the linearization of the mean-field evolution of the macroscopic variables in (9) and ancillary variables in (14) about the DFE is given by

$$\begin{aligned}
\dot{y}_d =& -\mu y_d + \lambda\langle a\rangle_d \eta[(1+\theta\tfrac{1-\eta}{\eta})y_d + (1-\theta)y_c] \\
&+ \lambda\eta[(1+\theta\tfrac{1-\eta}{\eta})z_d + (1-\theta)z_c], && \text{(15a)}\\
\dot{y}_c =& -\mu y_c + \lambda\langle a\rangle_c \tfrac{(1-\eta)\nu}{\gamma+nu}[(1+\tfrac{\theta\eta}{1-\eta})y_c + (1-\theta)y_d] \\
&+ \lambda\tfrac{(1-\eta)\nu}{\gamma+\nu}[(1+\tfrac{\theta\eta}{1-\eta})z_c + (1-\theta)z_d], && \text{(15b)}\\
\dot{z}_d =& -\mu z_d + \lambda\langle a^2\rangle_d \eta[(1+\theta\tfrac{1-\eta}{\eta})y_d + (1-\theta)y_c] \\
&+ \lambda\langle a\rangle_d \eta[(1+\theta\tfrac{1-\eta}{\eta})z_d + (1-\theta)z_p], && \text{(15c)}\\
\dot{z}_c =& -\mu z_c + \lambda\langle a^2\rangle_d \tfrac{(1-\eta)\nu}{\gamma+nu}[(1+\tfrac{\theta\eta}{1-\eta})y_c + (1-\theta)y_d] \\
&+ \lambda\langle a\rangle_c \tfrac{(1-\eta)\nu}{\gamma+\nu}[(1+\tfrac{\theta\eta}{1-\eta})z_p + (1-\theta)z_d], && \text{(15d)}\\
\dot{y}_p =& \gamma(1-\eta-y_c-y_p) - \nu y_p + \mu y_c. && \text{(15e)}
\end{aligned}$$

where

$$\langle a^m\rangle_d = \frac{1}{n_d}\sum\nolimits_{c\in\mathcal{V}_d} a_v^m, \quad \langle a^m\rangle_c = \frac{1}{n_c}\sum\nolimits_{c\in\mathcal{V}_c} a_v^m, \tag{16}$$

with $m \in \mathbb{Z}_{>0}$ being the m-order moments of the activity of deniers and cautious individuals, respectively.

From Proposition 3, we conclude that stability of the DFE for a heterogeneous ADN is determined by the four-dimensional block of the Jacobian matrix of (15) associated with the first four rows. In Fig. 4, we perform a parametric study to investigate how heterogeneity affects the epidemic threshold. We compare the epidemic threshold computed numerically for a heterogeneous ADN with the one computed analytically for a homogeneous ADN with the same average activity. Our results suggest that heterogeneity in the population tends to favor the spread of epidemic diseases. On the one hand, a strong decrease in the threshold is always recorded when deniers are more socially active than cautious individuals. On the other hand, if deniers are less active, we do not register the opposite, beneficial phenomenon.

V. Conclusion

We proposed a novel epidemic model on temporal networks that accounts for different behavioral responses of the population to the epidemic spreading. The model is parsimonious, and it relies mostly on parameters with a clear physical, epidemiological, or sociological interpretation, which can be obtained from the literature. By implementing our model using the ADN paradigm, we developed an analytically tractable

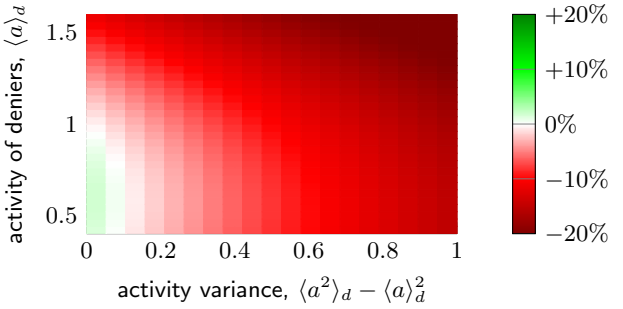

Fig. 4: Relative change in the epidemic threshold σ computed numerically using (15) with respect to the one of homogeneous ADNs (from (12)), as a function of the average activity of deniers and activity variance. Common parameters are $\theta = \eta = \gamma = 0.2$, $\nu = 0.5$, and average activity $\langle a \rangle = 1$. We set the activity variance of deniers equal to the one of cautious individuals ($\langle a^2 \rangle_d - \langle a \rangle_d^2 = \langle a^2 \rangle_c - \langle a \rangle_c^2$).

framework to evaluate the impact of deniers on the spread of an epidemic disease. Employing a mean-field approach and extending it to account for heterogeneity in the population behavioral response, we derived a closed-form expression for the epidemic threshold. Through its analysis, we exposed how deniers might have a strong impact on the epidemic spreading, especially in highly-polarized population. In such a scenario, a small minority of deniers is able to jeopardize massive efforts by public health authorities placed in awareness campaigns to curb the epidemic spreading.

Our results pave the way for several directions of future research. The theoretical results established in this letter are limited to the epidemic threshold for homogeneous ADNs. Further theoretical extensions may be pursued. First, a complete analysis of the three-dimensional nonlinear system of ODEs in Proposition 2 beyond the stability of the DFE may shed light on the role of deniers in endemic diseases. Second, studying linear stability conditions for the five-dimensional system in Proposition 3 may generate new theoretical insight to corroborate our numerical findings on the detrimental role of heterogeneity toward curbing an epidemic outbreak. Besides these theoretical developments, several modeling extensions are envisaged of our future research. For instance, non-ideal efficacy of self-protective behaviors should be incorporated through the inclusion of a contagion mechanism for individuals who adopt self-protective behaviors, with a suitable parameter to re-scale the infection probability [11]. Likewise, more complex and realistic decision-making mechanisms can be incorporated, such as those based on game theory [27], [28] or on opinion dynamics [29] and, besides awareness campaigns, we could study isolation of infected individuals [19] and the implementation of vaccination campaigns [7]. Finally, validation of the modeling framework against real-world epidemic data, such as those on the COVID-19 pandemic, is a key objective of the future research.

REFERENCES

[1] R. Pastor-Satorras, C. Castellano, P. Van Mieghem, and A. Vespignani, "Epidemic processes in complex networks," *Rev. Mod. Phys.*, vol. 87, pp. 925–979, 2015.

[2] C. Nowzari, V. M. Preciado, and G. J. Pappas, "Analysis and control of epidemics: a survey of spreading processes on complex networks," *IEEE Control Syst. Mag.*, vol. 36, no. 1, pp. 26–46, 2016.

[3] W. Mei, S. Mohagheghi, S. Zampieri, and F. Bullo, "On the dynamics of deterministic epidemic propagation over networks," *Annu. Rev. Contr.*, vol. 44, pp. 116–128, 2017.

[4] P. E. Paré, C. L. Beck, and T. Başar, "Modeling, estimation, and analysis of epidemics over networks: An overview," *Annu. Rev. Control*, vol. 50, pp. 345–360, 2020.

[5] L. Zino and M. Cao, "Analysis, prediction, and control of epidemics: A survey from scalar to dynamic network models," *IEEE Circuits Syst. Mag.*, vol. 21, no. 4, pp. 4–23, 2021.

[6] M. Ye and B. D. O. Anderson, "Competitive epidemic spreading over networks," *IEEE Control Syst. Lett.*, vol. 7, pp. 545–552, 2023.

[7] V. M. Preciado, M. Zargham, C. Enyioha, A. Jadbabaie, and G. Pappas, "Optimal vaccine allocation to control epidemic outbreaks in arbitrary networks," in *52nd IEEE Conf. Decis. Control*, 2013, pp. 7486–7491.

[8] G. Giordano *et al.*, "Modelling the COVID-19 epidemic and implementation of population-wide interventions in Italy," *Nat. Med.*, vol. 26, pp. 855–860, 2020.

[9] F. Della Rossa *et al.*, "A network model of Italy shows that intermittent regional strategies can alleviate the COVID-19 epidemic," *Nat. Comm.*, vol. 11, no. 1, p. 5106, 2020.

[10] R. Carli, G. Cavone, N. Epicoco, P. Scarabaggio, and M. Dotoli, "Model predictive control to mitigate the COVID-19 outbreak in a multi-region scenario," *Annu. Rev. Control*, vol. 50, pp. 373–393, 2020.

[11] F. Parino, L. Zino, M. Porfiri, and A. Rizzo, "Modelling and predicting the effect of social distancing and travel restrictions on COVID-19 spreading," *J. R. Soc. Interface*, vol. 18, no. 175, p. 20200875, 2021.

[12] J. J. Van Bavel *et al.*, "Using social and behavioural science to support COVID-19 pandemic response," *Nat. Hum. Behav.*, vol. 4, no. 5, pp. 460–471, 2020.

[13] C. Atchison *et al.*, "Early perceptions and behavioural responses during the COVID-19 pandemic: a cross-sectional survey of UK adults," *BMJ Open*, vol. 11, no. 1, 2021.

[14] S. Kleitman *et al.*, "To comply or not comply? a latent profile analysis of behaviours and attitudes during the COVID-19 pandemic," *PLOS ONE*, vol. 16, no. 7, pp. 1–22, 07 2021.

[15] J. Lang, W. Erickson, J.-S. Zhuo, "#MaskOn! #MaskOff! Digital polarization of mask-wearing in the United States during COVID-19," *PLOS ONE*, vol. 16, no. 4, pp. e0250817, 2021.

[16] A. Bessi *et al.*, "Homophily and polarization in the age of misinformation," *Eur. Phys. J.: Spec. Top.*, vol. 225, pp. 2047–59, 2016.

[17] L. Zino, A. Rizzo, and M. Porfiri, "Continuous-time discrete-distribution theory for activity-driven networks," *Phys. Rev. Lett.*, vol. 117, 2016.

[18] N. Perra, B. Gonçalves, R. Pastor-Satorras, and A. Vespignani, "Activity driven modeling of time varying networks," *Sci. Rep.*, vol. 2, 2012.

[19] L. Zino, A. Rizzo, and M. Porfiri, "On assessing control actions for epidemic models on temporal networks," *IEEE Control Syst. Lett.*, vol. 4, no. 4, pp. 797–802, 2020.

[20] F. D. Sahneh and C. Scoglio, "Epidemic spread in human networks," in *50th IEEE Conf. Dec. Control and Eur. Control. Conf.*, Dec 2011, pp. 3008–3013.

[21] V. M. Preciado, F. D. Sahneh, and C. Scoglio, "A convex framework for optimal investment on disease awareness in social networks," in *IEEE Global Conf. Signal. Inf. Process.*, 2013, pp. 851–854.

[22] P. V. Mieghem, J. Omic, and R. Kooij, "Virus spread in networks," *IEEE/ACM Trans. Netw.*, vol. 17, no. 1, pp. 1–14, Feb 2009.

[23] D. A. Levin, Y. Peres, and E. L. Wilmer, *Markov chains and mixing times*. Providence RI, US: American Mathematical Society, 2006.

[24] N. T. J. Bailey, *The Elements of Stochastic Processes with Applications to the Natural Sciences*. John Wiley & Sons, 1990.

[25] T. G. Kurtz, "Solutions of ordinary differential equations as limits of pure jump Markov processes," *J. Appl. Probab.*, vol. 7, no. 1, pp. 49–58, 1970.

[26] W. Rugh, *Linear System Theory*. Prentice Hall, 1996, vol. 2.

[27] A. R. Hota, T. Sneh, and K. Gupta, "Impacts of game-theoretic activation on epidemic spread over dynamical networks," *SIAM J. Control Optim.*, vol. 60, no. 2, pp. S92–S118, 2022.

[28] K. Frieswijk, L. Zino, M. Ye, A. Rizzo, and M. Cao, "A mean-field analysis of a network behavioral–epidemic model," *IEEE Control Syst. Lett.*, vol. 6, pp. 2533–2538, 2022.

[29] B. She, J. Liu, S. Sundaram, and P. E. Pare, "On a networked SIS epidemic model with cooperative and antagonistic opinion dynamics," *IEEE Trans. Control Netw. Syst.*, pp. 1–1, 2022.